

# Frequency modulation spectroscopy with a THz quantum-cascade laser

R. Eichholz,<sup>1,\*</sup> H. Richter,<sup>1</sup> M. Wienold,<sup>2</sup> L. Schrottke,<sup>2</sup> R. Hey,<sup>2</sup> H. T. Grahn,<sup>2</sup>  
and H.-W. Hübers<sup>1,3</sup>

<sup>1</sup>*Institute of Planetary Research, German Aerospace Center (DLR), Rutherfordstr. 2, 12489 Berlin, Germany*

<sup>2</sup>*Paul-Drude-Institut für Festkörperelektronik, Hausvogteiplatz 5–7, 10117 Berlin, Germany*

<sup>3</sup>*Institut für Optik und Atomare Physik, Technische Universität Berlin, Straße des 17. Juni 135, 10623 Berlin, Germany*

\*[rene.eichholz@dlr.de](mailto:rene.eichholz@dlr.de)

**Abstract:** We report on a terahertz spectrometer for high-resolution molecular spectroscopy based on a quantum-cascade laser. High-frequency modulation (up to 50 MHz) of the laser driving current produces a simultaneous modulation of the frequency and amplitude of the laser output. The modulation generates sidebands, which are symmetrically positioned with respect to the laser carrier frequency. The molecular transition is probed by scanning the sidebands across it. In this way, the absorption and the dispersion caused by the molecular transition are measured. The signals are modeled by taking into account the simultaneous modulation of the frequency and amplitude of the laser emission. This allows for the determination of the strength of the frequency as well as amplitude modulation of the laser and of molecular parameters such as pressure broadening.

©2013 Optical Society of America

**OCIS codes:** (140.5965) Semiconductor lasers, quantum cascade; (140.3518) Lasers, frequency modulated; (260.3090) Infrared, far; (300.6380) Spectroscopy, modulation; (300.6495) Spectroscopy, terahertz.

---

## References and links

1. D. M. Mittelman, R. H. Jacobsen, R. Neelamani, R. G. Baraniuk, and M. C. Nuss, "Gas sensing using terahertz time-domain spectroscopy," *Appl. Phys. B* **67**(3), 379–390 (1998).
2. C. Bauer, A. K. Sharma, U. Willer, J. Burgmeier, B. Braunschweig, W. Schade, S. Blaser, L. Hvozدارa, A. Müller, and G. Holl, "Potentials and limits of mid-infrared laser spectroscopy for the detection of explosives," *Appl. Phys. B* **92**(3), 327–333 (2008).
3. P. Werle, "A review of recent advances in semiconductor laser based gas monitors," *Spectrochim. Acta A* **54**(2), 197–236 (1998).
4. I. Linnerud, P. Kaspersen, and T. Jaeger, "Gas monitoring in the process industry using diode laser spectroscopy," *Appl. Phys. B* **67**(3), 297–305 (1998).
5. S. Heyminck, U. U. Graf, R. Güsten, J. Stutzki, H.-W. Hübers, and P. Hartogh, "GREAT: the SOFIA high-frequency heterodyne instrument," *Astron. Astrophys.* **542**, L1 (2012).
6. G. C. Bjorklund, "Frequency-modulation spectroscopy: a new method for measuring weak absorptions and dispersions," *Opt. Lett.* **5**(1), 15–17 (1980).
7. D. E. Cooper and R. E. Warren, "Frequency modulation spectroscopy with lead-salt diode lasers: a comparison of single-tone and two-tone techniques," *Appl. Opt.* **26**(17), 3726–3732 (1987).
8. G. C. Bjorklund, M. D. Levenson, W. Lenth, and C. Ortiz, "Frequency modulation (FM) spectroscopy," *Appl. Phys. B* **32**(3), 145–152 (1983).
9. L.-G. Wang, D. A. Tate, H. Riris, and T. F. Gallagher, "High-sensitivity frequency-modulation spectroscopy with a GaAlAs diode laser," *J. Opt. Soc. Am. B* **6**(5), 871–876 (1989).
10. S. Borri, S. Bartalini, P. De Natale, M. Inguscio, C. Gmachl, F. Capasso, D. L. Sivco, and A. Y. Cho, "Frequency modulation spectroscopy by means of quantum-cascade lasers," *Appl. Phys. B* **85**(2–3), 223–229 (2006).
11. H.-W. Hübers, R. Eichholz, S. G. Pavlov, and H. Richter, "High resolution terahertz spectroscopy with quantum cascade lasers," *J. Infrared Millimeter Terahertz Waves* **34**(5–6), 325–341 (2013).
12. C. Sirtori, S. Barbieri, and R. Colombelli, "Wave engineering with THz quantum cascade lasers," *Nat. Photonics* **7**(9), 691–701 (2013).

13. H.-W. Hübers, S. G. Pavlov, H. Richter, A. D. Semenov, L. Mahler, A. Tredicucci, H. E. Beere, and D. A. Ritchie, "High-resolution gas phase spectroscopy with a distributed feedback terahertz quantum cascade laser," *Appl. Phys. Lett.* **89**(6), 061115 (2006).
14. R. Eichholz, H. Richter, S. G. Pavlov, M. Wienold, L. Schrottke, R. Hey, H. T. Grahn, and H.-W. Hübers, "Multi-channel terahertz grating spectrometer with quantum-cascade laser and microbolometer array," *Appl. Phys. Lett.* **99**(14), 141112 (2011).
15. L. Consolino, S. Bartalini, H. E. Beere, D. A. Ritchie, M. S. Vitiello, and P. De Natale, "THz QCL-based cryogen-free spectrometer for in situ trace gas sensing," *Sensors* **13**(3), 3331–3340 (2013).
16. M. Gehrtz, W. Lenth, A. T. Young, and H. S. Johnston, "High-frequency-modulation spectroscopy with a lead-salt diode laser," *Opt. Lett.* **11**(3), 132–134 (1986).
17. W. Lenth, "High frequency heterodyne spectroscopy with current-modulated diode lasers," *IEEE J. Quantum Electron.* **20**(9), 1045–1050 (1984).
18. H. Richter, M. Greiner-Bär, S. G. Pavlov, A. D. Semenov, M. Wienold, L. Schrottke, M. Giehler, R. Hey, H. T. Grahn, and H.-W. Hübers, "A compact, continuous-wave terahertz source based on a quantum-cascade laser and a miniature cryocooler," *Opt. Express* **18**(10), 10177–10187 (2010).
19. W. C. B. Peatman, P. A. D. Wood, D. Porterfield, T. W. Crowe, and M. J. Rooks, "Quarter-micrometer GaAs Schottky barrier diode with high video responsivity at 118  $\mu\text{m}$ ," *Appl. Phys. Lett.* **61**(3), 294–296 (1992).

## 1. Introduction

Laser-based spectroscopy for the detection and monitoring of trace gases is established for many regions of the electromagnetic spectrum with applications in biochemical, environmental, astronomical, industrial, and security sensing [1–5]. In particular for infrared wavelengths, a number of different spectroscopic techniques for high-resolution molecular spectroscopy have been developed, since this is the region where many molecules have characteristic spectra.

Wavelength and frequency modulation techniques are frequently used for improving the detection sensitivity in laser absorption spectrometers [6–8]. In both cases, the frequency of the laser is modulated by some means, for example by using an external acousto-optical modulator or by modulating the driving current of the laser. The laser radiation is detected with the modulation frequency as a reference, for example with a lock-in amplifier (LIA) or a heterodyne detector. In infrared spectroscopy, the term *wavelength modulation* is used when the modulation frequency is smaller than the width of the investigated molecular absorption line. When the modulation frequency is larger than the line width, the technique is called *frequency modulation* (FM), which was first introduced in 1980 by G. Bjorklund [6]. Both techniques are two limiting cases of the same general approach. The advantage of FM is that limitations by low-frequency noise of the laser can be overcome if the modulation frequency is sufficiently large. At infrared and visible wavelengths, detector-limited sensitivities as low as  $10^{-7}$ – $10^{-10}$  have been demonstrated with FM spectroscopy and lead-salt or GaAlAs diode lasers [3, 9]. More recently, the technique was extended to an infrared quantum-cascade laser (QCL) [10].

High-resolution terahertz (THz) spectroscopy is a powerful tool, not only for research, but also for trace gas sensing, environmental monitoring, and security. At THz frequencies, QCLs are promising sources for high-resolution, high-sensitivity spectroscopy [11]. These lasers are powerful as well as frequency tunable, and they exhibit a narrow line width [12]. High-resolution molecular spectroscopy has been demonstrated using a distributed feedback (DFB) THz QCL [13]. Frequency tunability of a few GHz was accomplished by varying the current and the temperature of the QCL. The limited frequency coverage of DFB QCLs can be overcome by using a multimode laser and by imaging the modes onto a microbolometer camera [14]. The baseline slope, which appears in direct absorption spectroscopy due to the non-linear light-current dependence of the QCL, can be eliminated either by appropriate modulation techniques or by a differential technique with a reference detector [15]. All of these approaches have in common that they use either direct detection of the QCL radiation or wavelength modulation.

In this article, we describe a THz absorption spectrometer for high-resolution molecular spectroscopy employing FM. The spectrometer is based on a QCL and a Schottky diode as

the detector. The modulation parameters, which are characteristic of the QCL, are determined, and initial molecular spectroscopy results are presented.

## 2. Theoretical background

A straightforward experimental setup for implementing FM spectroscopy consists of a laser, an absorption cell, a detector, and a LIA. The radiation from the laser passes through the cell, which contains the molecule of interest, and then impinges on a fast detector. By modulating the laser frequency, standard lock-in techniques allow for the detection of the signal at the modulation frequency. Molecular absorption lines at THz frequencies are typically a few MHz wide if Doppler broadening prevails, while pressure broadening dominates at moderate pressures of a few hPa with line widths of a few tens of MHz. Therefore, FM spectroscopy requires modulation frequencies of several 10 MHz, and the detector as well as the LIA have to be able to comply with these frequencies.

FM can be realized with a THz QCL by modulating its driving current. However, the current modulation causes not only FM, but also amplitude modulation (AM) of the laser emission. In this case, the electric field is described by [16, 17]

$$E(t) = E_0 [1 + M \sin(\omega_m t + \Psi) \exp[i \omega_0 t + i \beta \sin(\omega_m t)]], \quad (1)$$

where  $E_0$  and  $\omega_0$  denote the laser field and carrier frequency,  $\omega_m$  the modulation frequency,  $M$  the AM index,  $\beta$  the FM index, and  $\Psi$  the phase difference between AM and FM. If  $M$  and  $\beta$  are small, the laser field consists of a strong carrier at a frequency  $\omega_0$  and two weak sidebands at  $\omega_{\pm 1} = \omega_0 \pm \omega_m$ .

Provided that the absorption loss and phase shift caused by the molecule in the absorption cell are small, the combination of FM and AM yields the following expression for the laser intensity impinging on the detector [8, 16, 17]:

$$I(t) \sim I_0 \left[ 1 + \beta (\delta_{-1} - \delta_1) \cos(\omega_m t) + M (2 - 2\delta_0 - \delta_{-1} - \delta_1) \sin(\omega_m t + \Psi) + M (\Phi_{-1} - \Phi_1) \cos(\omega_m t + \Psi) + \beta (\Phi_{-1} + \Phi_1 + 2\Phi_0) \sin(\omega_m t) \right], \quad (2)$$

where  $\delta_0$  and  $\delta_{\pm 1}$  describe the amplitude attenuation and  $\Phi_0$  and  $\Phi_{\pm 1}$  describe the phase shifts at the frequencies  $\omega_0$  and  $\omega_{\pm 1}$ , respectively. The signal consists of an in-phase component ( $\sim \cos \omega_m t$ ) and a quadrature component ( $\sim \sin \omega_m t$ ) which can be detected by the LIA. By adjusting the phase at the LIA properly, one or more of the four time-varying terms in Eq. (2) can be selected. For example if  $\Psi = 0$  or  $\pi/2$ , pure absorption and phase signals can be extracted, while in the general case of  $\Psi \neq 0$  or  $\pi/2$  the recorded signal will contain contributions from absorption loss and phase shift.

Figure 1 shows the calculated in-phase and quadrature signals obtained at the output of the LIA for pure FM and pure AM. They were calculated for a modulation frequency of 50 MHz and an absorption profile, which is described by a Lorentz function with a full width at half maximum (FWHM) of 14 MHz. In the case of pure FM, the in-phase signal of the LIA has two absorption features with opposite sign, odd symmetry, and zero background as shown Fig. 1(a). By increasing the laser frequency, first the upper FM sideband probes the absorption line, which leads to a positive signal. At a separation of  $2\omega_m = 100$  MHz the lower sideband probes the absorption line, and a negative signal appears. The shape of both signals resembles the shape of the absorption line. The quadrature signal shown in Fig. 1(b) has a dispersion-like shape with three overlapping components, which belong to both sidebands and the carrier frequency. Again, the symmetry is odd, and the baseline is zero. The AM line shapes are significantly different. The in-phase signal shown in Fig. 1(c) contains three absorption signals on a positive background. Two of them at  $\pm 50$  MHz are generated by the sidebands, while the center one is due to the carrier. The quadrature signal shown in Fig. 1(d)

contains two overlapping curves, which occur when the upper sideband and then the lower sideband are swept through the resonance.

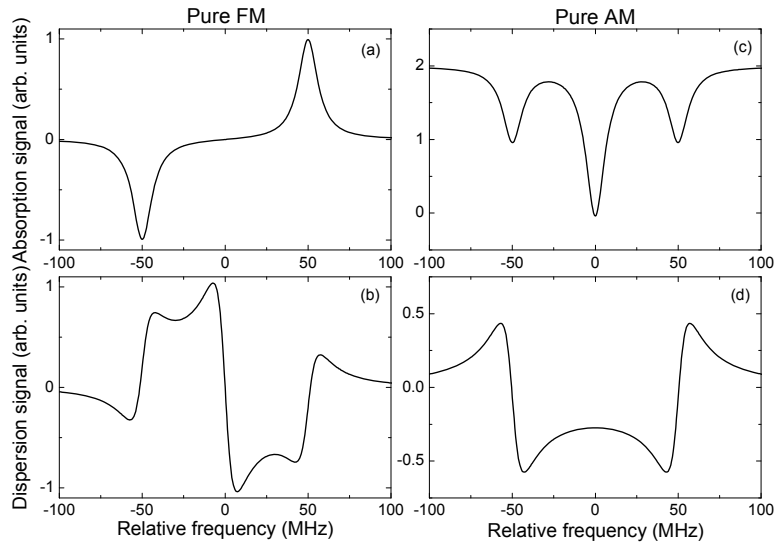


Fig. 1. Calculated line shapes of a molecular absorption line with a Lorentzian profile with 14 MHz FWHM at a modulation frequency of 50 MHz. (a) In-phase and (b) quadrature signal for pure FM. (c) In-phase and (d) quadrature signal for pure AM.

### 3. Experimental setup

The setup of the spectrometer is shown in Fig. 2. The active region of the QCL is based on a hybrid design, which uses an intersubband transition resonant to the longitudinal optical phonon for efficient carrier injection. The laser emits at 3.1 THz and has a 1.16 mm long Fabry-Pérot cavity and a single-plasmon waveguide. Both facets of the cavity are uncoated.

The QCL was fixed with indium onto a gold-plated copper submount and attached to another copper holder, which in turn was mounted the cold finger of a compact, air-cooled Stirling cooler (Ricor model K535) [18]. The QCL, copper mount, and the cold finger were encapsulated in a vacuum housing. The output window for the QCL radiation is made from high-density polyethylene (HDPE) and is tilted with respect to the optical axis in order to avoid standing waves and to minimize Fabry-Pérot type etalon effects in the setup and back reflections into the laser. The vacuum housing around the window was covered with Eccosorb™ in order to minimize standing waves and undesired reflections.

The driving current for the QCL was supplied by a commercially available current source (ILX model LDX-3232). The emission spectrum of the QCL contains several modes with a spacing of about 26 GHz as measured with a Fourier transform spectrometer (Bruker model Vertex 80V). The output power of the QCL was 1 mW at a current of 550 mA and a temperature of 45 K. The beam of the QCL was collimated with a lens made from polymethylpentene (TPX®) and guided through an absorption cell. An off-axis parabolic mirror was used to focus the radiation onto the Schottky diode. The absorption cell was 31 cm long and has 1 mm thick windows made from HDPE. Both were tilted with respect to the optical axis in order to minimize standing waves. The pressure inside the cell was measured with a capacitive manometer. The Schottky diode is made from GaAs and equipped with an open structure corner cube antenna [19]. Fine tuning of the QCL frequency was achieved by tuning the driving current or the heat sink temperature. A maximum tuning range of approximately 3 GHz was obtained for each of the laser modes.

The driving current of the QCL was superimposed with a small sinusoidal current with a modulation frequency up to 50 MHz, using a bias-tee. The modulation current was generated

by a LIA (Zurich Instruments model HF2LI). We used modulation amplitudes up to 4 mA corresponding to a frequency modulation of up to 32 MHz, which is nearly equal to the FWHM of the CH<sub>3</sub>OH absorption lines at a pressure of 1 hPa. The signal from the Schottky diode was detected with the same LIA. A computer was used to control the QCL driving current as well as the data acquisition.

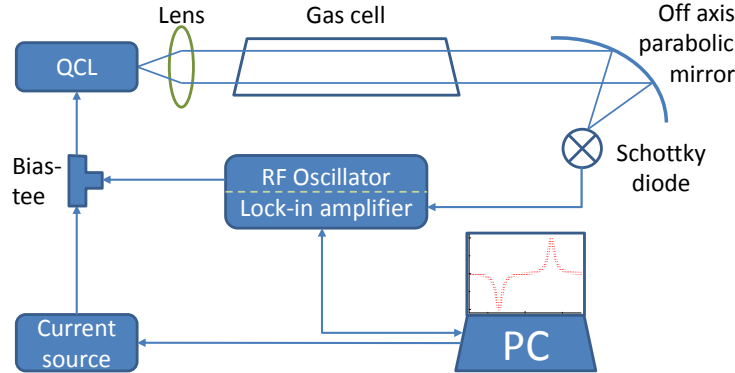


Fig. 2. Block diagram of the spectrometer with frequency modulation spectroscopy.

#### 4. Experimental results

As an example of the spectrum measured with FM spectroscopy at a modulation frequency of 50 MHz, the corresponding in-phase and quadrature signals are shown in Fig. 3. Three absorption lines are visible in the about 1.5 GHz wide frequency range. The spectrum was measured by tuning the QCL current in steps of 0.5 mA (corresponding to approximately 6 MHz). The absolute frequency calibration was done by a comparison with a CH<sub>3</sub>OH spectrum, which also allows for the determination of the frequency tuning of the QCL which is approximately 8 MHz/mA. Note that the tuning is not perfectly linear if a wide current range is considered. However, for a small current range which covers just a single absorption line the linearity is excellent [11]. The integration time of the LIA was 47 ms for each spectral resolution element, resulting in a total measurement time for the whole frequency range of about 17 s. The frequency tuning rate in terms of current is much higher than the temperature-induced frequency tuning ( $\sim 100$  MHz/K), if a 1.5-GHz wide spectral scan is considered. During one scan the temperature increases by 0.4 K. Therefore, it is safe to assume that for a single absorption line the frequency change originates only from the current tuning, while temperature tuning due to heating of the QCL by the current is negligible. For this measurement, the phase at the LIA was set to a value to obtain pure absorption and dispersion signals in the in-phase and quadrature channels, respectively, of the LIA.

Fitting Eq. (2) to the measured spectrum of a single absorption line allows for the determination of several characteristic parameters of the QCL and the molecule under investigation. With respect to the QCL, the AM index  $M$  and the FM index  $\beta$  can be determined. With respect to the molecule parameters such as, the frequency and the line width of the transition can be determined.

Figure 4 shows an absorption line of CH<sub>3</sub>OH measured at a pressure of 1 hPa using FM spectroscopy along with the corresponding fit of Eq. (2). The current amplitude of the modulation was set to 1.6 mA, which translates into a 15 MHz frequency modulation. The phase of the LIA was adjusted in such a way that the absorption and the dispersion contribution to the FM signal appear purely in the in-phase and quadrature signals, respectively.

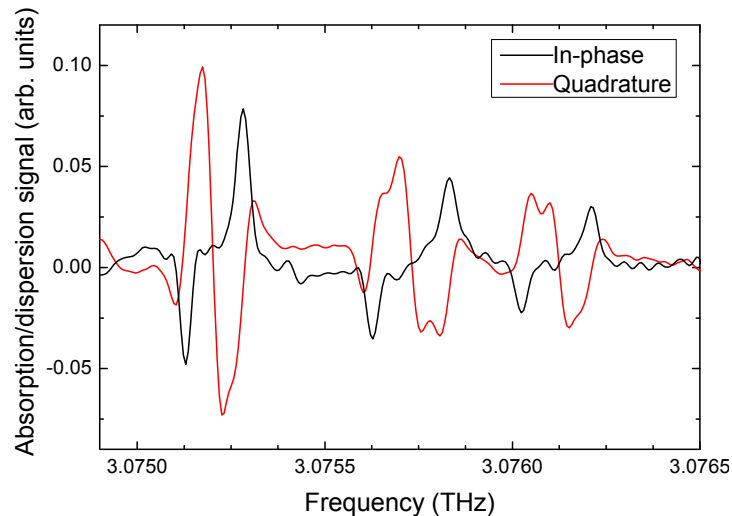


Fig. 3. Typical FM spectra of  $\text{CH}_3\text{OH}$  at around 3.0758 THz. The spectrum was obtained by sweeping the driving current of the QCL. Frequency calibration was done by comparison with a  $\text{CH}_3\text{OH}$  spectrum measured with a FTIR. The phase of the LIA was chosen in order to obtain the absorption signal as the in-phase component and the dispersion signal as the quadrature component of the LIA output.

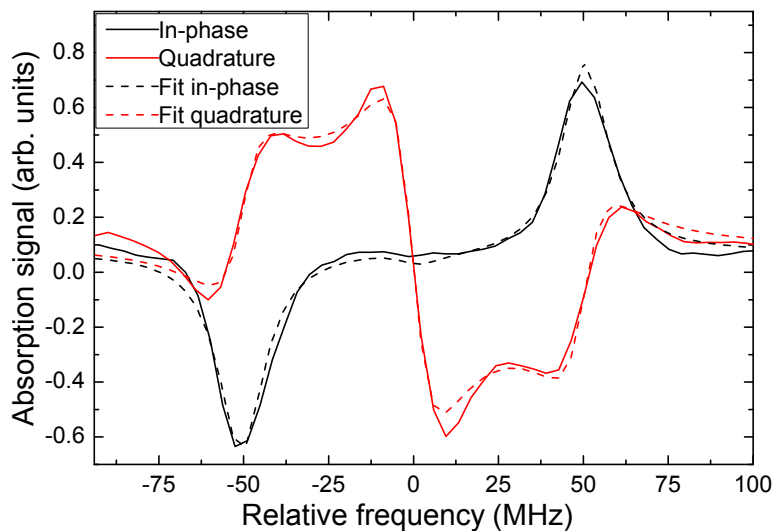


Fig. 4. Measured and fitted data for the in-phase and quadrature term of an absorption line with FM spectroscopy with a 50 MHz modulation frequency at a carrier frequency of 3.0752 THz. The features for the in-phase measurement are separated by 100 MHz.

The spacing between the two peaks in the in-phase signal corresponds to  $2\omega_m$ . The peak occurs, because when increasing the frequency of the QCL the upper FM sideband probes the absorption line first (feature at + 50 MHz in Fig. 4). The second feature appears at -50 MHz when the lower FM sideband passes the absorption line. The opposite sign of the two peaks is typical for FM modulation (cf. Figure 1). The quadrature signal shows the three characteristic features of the dispersion signal of FM [cf. Figure 1(b)]. The central one appears when the carrier frequency is in resonance with the absorption line, while the other two appear when the upper and the lower sidebands are in resonance.

The spacing of 100 MHz between the main peaks of the in-phase signal can be used to calibrate the frequency-current dependence of the QCL around an absorption line with high accuracy. A limitation is given by the linewidth of the molecular transition. This is illustrated in Fig. 5, which shows the measured line shapes for different modulation frequencies ranging from 1 up to 50 MHz. Almost no change of the peak position occurs in the lower frequency range up to approximately 10 MHz. Once the modulation frequency is significantly larger than the FWHM of the line, the separation of the two features approaches  $2\omega_m$ .

The values of  $M$ ,  $\beta$ , and  $\Psi$  are characteristic for a particular type of laser. The fit according to Eq. (2) allows for the determination of the ratio of the amplitude and frequency modulation index  $M$  and  $\beta$ , but not of each value separately. The result for the line shown in Fig. 4 is  $M/\beta = 0.07 \pm 0.03$ . This demonstrates that FM dominates and AM contributes little to the signal. This is expected because the change of the output power of the QCL is less than 1% for a modulation with 1.6 mA at 540 mA. The FM at 1.6 mA is 15 MHz, which leads to an almost complete modulation of the absorption line, i.e. a change of the transmitted power of about 10% at 1 hPa. Reported ratios for lead-salt laser diodes operating at 8  $\mu\text{m}$  and 10  $\mu\text{m}$  are quite similar with values of 0.12 [15] and 0.07–0.15 [7].

In order to separately determine  $M$  and  $\beta$ , we measured the signal-to-noise ratio (SNR) at the maximum of the absorption line as a function of the FM index  $\beta$  by varying the amplitude of the modulation current from 50  $\mu\text{A}$  to 4 mA. According to the calculation in [7], Cooper et al. reported that the best sensitivity should be obtained for a frequency modulation index of about 1.15. The optimum value for  $\beta$  depends on  $M$  and on the line width of the molecule. In general, it corresponds to an FM of approximately one FWHM. In our experiment, the best SNR at a pressure of 40 Pa and a modulation frequency of 50 MHz was achieved with a current modulation of about 1.8 mA. This implies an FM index  $\beta$  of about 1.15 at 1.8 mA and about 1 at 1.6 mA. From the latter value, we derive an AM index  $M$  of about 0.07.

Measurements using various phase settings for the LIA revealed that the FM/AM phase shift  $\Psi$  varies between  $-\pi$  and  $\pi$ . This is similar to what has been observed for lead-salt laser diodes [7], but different from other results, where a constant phase was measured [16, 17].

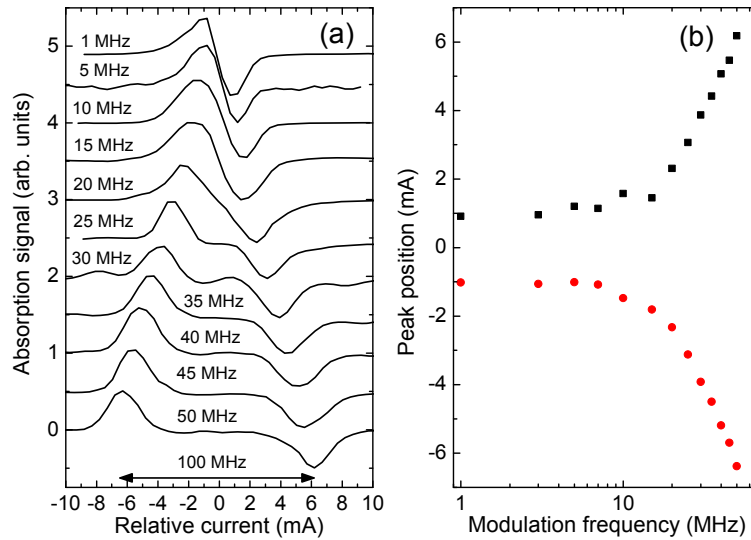


Fig. 5. (a) Experimental FM absorption line shapes for different modulation frequencies (offset for clarity). The FWHM of the transition line is 28 MHz. (b) Peak position as a function of modulation frequency.

As another test, we measured the line width of the  $\text{CH}_3\text{OH}$  line at 3.0752 THz as a function of pressure in the range from 20 to 180 Pa with a modulation frequency of 50 MHz.

Figure 6 shows the measured line widths for the in-phase and the quadrature component as a function of pressure. The measurement displays a linear dependence across the whole pressure range. The measured pressure broadening is similar for both channels with an average value of  $(339 \pm 9)$  kHz/Pa, which agrees well with literature values [12]. The Doppler width determined from the fits is  $(5.6 \pm 0.6)$  MHz, which is in good agreement with the expected Doppler width of 6.7 MHz.

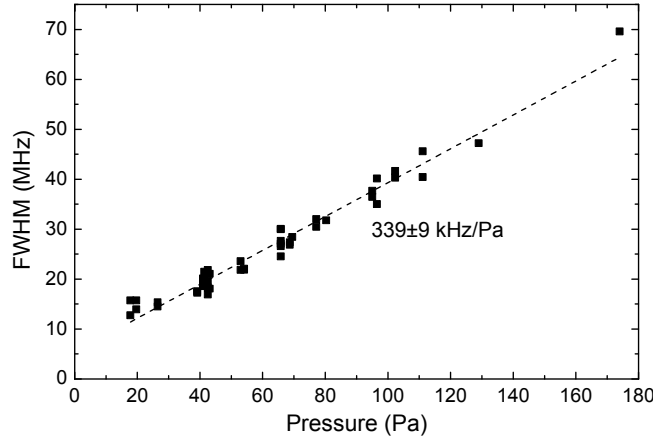


Fig. 6. FWHM of the  $\text{CH}_3\text{OH}$  transition as a function of pressure in the absorption cell.

## 5. Summary and conclusions

In summary, we have realized a THz absorption spectrometer for high-resolution molecular spectroscopy with a frequency-modulated QCL. FM is achieved by superimposing a small AC current on the DC driving current of the laser. Since current modulation also changes the output power of the laser, the signal is not purely frequency modulated, but contains a small contribution from AM. The obtained spectra are well described assuming dominating FM. The observed FM and AM indices  $\beta$  and  $M$  confirm that the contribution of AM is rather small with a ratio  $M/b$  of approximately 0.07. Finally, we measured the pressure broadening of a rotational transition of  $\text{CH}_3\text{OH}$  at 3.0752 THz and determined a value of 339 kHz/Pa. This demonstrates that FM is a technique which can be applied to high-resolution THz spectroscopy. In particular, the dispersion of a molecule can be investigated. Further studies have to be carried out in order to determine whether wavelength or frequency modulation is advantageous in terms of sensitivity.

## Acknowledgments

This work was supported in part by the European Commission through the ProFIT program of the Investitionsbank Berlin. R.E. acknowledges support by the Helmholtz Research School on Security Technologies.